drag coefficient minus the drag coefficient predicted by the theory in question for the conditions of the experiment, this difference being divided by the latter theoretical drag coefficient.

The "order of merit" of the various theories in respect to accuracy may be deduced from Fig. 1. Of the theories surveyed, the second theory of van Driest[1] proves to give the lowest rms proportional error, namely 11.0%.

The theories that were not included in this study were omitted either because they contained constants for which the authors of the theories had made no recommendation or because use of the theories would have involved an amount of computation which was an order of magnitude greater than that of the most complex theory included in this study, namely that of Kutateladze and Leont'ev.[2] It is of course possible that some of these omitted theories could give even lower rms errors than those represented in Fig. 1.

2. New Calculation Procedure

In an effort to reduce the rms error still further and to make the computation of drag under compressible turbulent conditions an easy one for the designer, a new procedure of calculation has been developed. The essential assumption is that the relations between drag coefficient and Reynolds number which are valid for uniform-property flow continue to hold when properties vary, provided that the drag coefficient is multiplied by a quantity F_c and that the Reynolds number is multiplied by a quantity $F_{R\delta}$ (if the Reynolds number is based on momentum thickness) or F_{Rx}, (if the Reynolds number is based on plate length). The various F's are functions of Mach number and temperature ratio alone.

It has been found that the rms value of the proportional error can be reduced to 9.9% if the following choices are made for the F's:

$$F_c = \left(\frac{T_S}{T_G}\right) \Big/ \left\{\frac{1}{a}\sin^{-1}\frac{2a^2 - b}{(4a^2 + b^2)^{1/2}} + \sin^{-1}\frac{b}{(4a^2 + b^2)^{1/2}}\right\}^2 \tag{1}$$

where

$$a^2 = \left(r\,\frac{\gamma - 1}{2}\,M_G^2\right) \Big/ \left(\frac{T_S}{T_G}\right)$$

$$b = \left[\left(1 + r\,\frac{\gamma - 1}{2}\,M_G^2\right) \Big/ \left(\frac{T_S}{T_G}\right)\right] - 1$$

M_G = mainstream Mach number

T_S = wall temperature, °R

T_G = mainstream temperature, °R

γ = specific heat ratio = 1.4 for air

r = recovery factor = 0.89 for Prandtl number $\approx$ 0.7

This function is of course similar to that appearing in the theories of van Driest[1, 3] and many others:

$$F_{R\delta} = T_S/T_G{}^{-0.702}(T_{ad,S}/T_S)^{0.788} \tag{2}$$

where $T_{ad,S}$ is the adiabatic wall temperature (°R). Also,

$$F_{Rx} = F_{R\delta}/F_c \tag{3}$$

The details of the work reported here, together with tables and charts of F_c, $F_{R\delta}$, and other useful functions, will be published elsewhere.[4]

References

[1] Van Driest, E. R., "The turbulent boundary layer with variable Prandtl number," *50 Years of Boundary Layer Theory*, edited by H. Görtler and W. Tollmien (1955), pp. 257–271.

[2] Kutateladze, S. S. and Leont'ev, A. I., "Drag law in a turbulent flow of a compressible gas and the method of calculating friction and heat transfer," *Discussion of Heat and Mass Transfer* (Akademiya Nauk Belorusskoi S.S.R., Minsk, 1961, pp. 1–23; also transl. TIL T5258 (1962).

[3] Van Driest, E. R., "Turbulent boundary layer in compressible fluids," J. Aeronaut. Sci. **18**, 145–160, 216 (1951).

[4] Spalding, D. B. and Chi, S. W., "The drag of a compressible turbulent boundary layer on a smooth flat plate with and without heat transfer," J. Fluid Mech. **17** (1963).

Contact Surface Tailoring in a Chemical Shock Tube

O. Trass* and D. Mackay†

University of Toronto, Toronto, Ontario, Canada

This paper presents a method of computing shock tube driver-gas compositions that will give tailoring conditions when the reflected shock wave passes through the contact surface. The method is suitable for any driven gas and any driver-gas mixture for which tailoring is possible. Tailoring data are given for mixtures of hydrogen or helium with argon or nitrogen driving argon. The effects of adding reactant gas to the argon are discussed.

Nomenclature

P = absolute pressure
T = absolute temperature
Cv = constant volume heat capacity per unit mass
E = $Cv \cdot T$, the internal energy per unit mass
γ = specific heat ratio Cp/Cv
α = $(\gamma + 1)/(\gamma - 1)$
β = $(\gamma - 1)/2\gamma$
X = mole fraction of the lower molecular weight component of the driver gas
P_{ij} = P_i/P_j
T_{ij} = T_j/T_j
E_{ij} = E_j/E_i

Subscripts correspond to the gas regions in Fig. 1.

Palmer and Knox[1] have published a useful table of conditions under which contact surface tailoring exists in a chemical shock tube with argon as the shocked gas and mixtures of He-A and N_2-H_2 as driver gases. It has been found that it is not always convenient to use such mixtures especially if the investigation involves analysis of the products of the gaseous reaction for a component present in the driver gas either in bulk or as an impurity. This paper extends the data given by Palmer and Knox to He-N_2 and H_2-A mixtures and indicates the method of solution of the tailoring equations for these and other gas mixtures. The method can be used for driven gases other than argon and for driven gas mixtures.

Computation of the driver-gas composition required to give a particular temperature in the reflected shock region and to give tailored conditions at the contact surface can be resolved into the solution of a number of simultaneous equations. If the specific heat ratios of the components of the driver gas are equal, for example H_2-N_2 or He-A, then solution is simple though tedious. If, however, they are unequal, the equations are implicit and only can be solved by a trial and error method feasible only on a computer.

Received June 5, 1963. This work was supported by a grant from the National Research Council, Ottawa, Canada. Computation was on the IBM 7090 of the Institute of Computer Science of the University of Toronto.

* Associate Professor, Department of Chemical Engineering and Applied Chemistry.

† National Research Council Post Doctoral Fellow, Department of Chemical Engineering and Applied Chemistry.

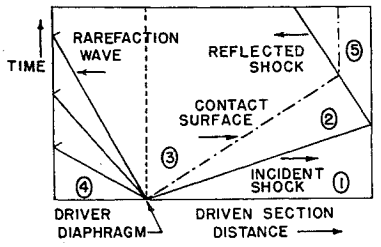

Fig. 1 Time-distance diagram for a simple shock tube.

Figure 1 shows the wave systems generated in a simple shock tube in the form of a time-distance diagram. The gas regions are numbered corresponding to the subscripts used in the equations below. For a more detailed discussion of the wave systems reference can be made to Glass and Hall.[2]

Glass and Hall[2] have shown that for a simple shock tube with ideal gases, assuming ideal diaphragm bursting and neglecting boundary-layer effects and shock wave attenuation, the following equations apply:

$$P_{41} = P_{21}\{1 - (P_{21} - 1)[\beta_4 E_{14}/(\alpha_1 P_{21} + 1)]^{1/2}\}^{-1/\beta_4} \quad (1)$$

$$P_{52} = (\alpha_1 P_{21} + 2P_{21} - 1)/(P_{21} + \alpha_1) \quad (2)$$

$$T_{21} = P_{21}(\alpha_1 + P_{21})/(\alpha_1 P_{21} + 1) \quad (3)$$

$$T_{52} = P_{52}(\alpha_1 + P_{52})/(\alpha_1 P_{52} + 1) \quad (4)$$

$$T_{43} = (P_{41}/P_{21})^{2\beta_4} \quad (5)$$

In addition, the condition for a tailored contact surface for the reflected shock passing from region 2 to region 3 is

$$E_{32} = Cv_3 T_3/Cv_2 T_2 = (\alpha_3 P_{52} + 1)/(\alpha_2 P_{52} + 1) \quad (6)$$

Normally T_1 and T_4 are equal, and the equations can be combined to give Eq. (7), which contains only P_{21} and the thermodynamic properties of the driven and driver gases:

$$\frac{Cv_4(1 + \alpha_1 P_{21})\{1 - (P_{21} - 1)[\beta_4 Cv_1/Cv_4(\alpha_1 P_{21} + 1)]^{1/2}\}^{-2}}{Cv_1 P_{21}(\alpha_1 + P_{21})} = \frac{\{\alpha_4 + (\alpha_1 + P_{21})/(\alpha_1 P_{21} + 2P_{21} - 1)\}}{\{\alpha_1 + (\alpha_1 + P_{21})/(\alpha_1 P_{21} + 2P_{21} - 1)\}} \quad (7)$$

Computing Procedure

Normally the driven gas consists of a few percent of the reactant gas in argon. The thermodynamic properties of both driven and driver gas can be estimated by weighting the individual specific heats in proportion to their weight fraction to obtain the specific heats of the mixtures and γ, α, and β deduced therefrom. The assumption that the driven gas behaves as argon may introduce serious errors especially if the reactant gas is present in appreciable quantities and has a high specific heat and a low specific heat ratio.

A P_{21} pressure ratio is chosen to correspond to the desired temperature using Eqs. (2–4). It now remains to find the driver-gas composition and the P_{41} bursting pressure ratio, which will give the desired P_{21} and produce tailoring. This can be done by programming a computer to take a value of X, the mole fraction of the lower molecular weight component of the driver, to deduce the corresponding values of Cv_4, γ_4, α_4, and β_4, and then compute both sides of Eq. (7) and determine the difference between them. The iterative procedure starts with X equal to zero and is repeated with X increasing by increments sufficiently small to give the accuracy required. When the difference between the two sides of Eq. (7) passes through zero, the corresponding value of X is within one incremental step of the exact solution, and the values of X and P_{41} can be printed out.

More convenient results can be obtained by computing a set of values of X and P_{41} corresponding to a series of P_{21} values for a given driven gas, and intermediate values can be interpolated.

Table 1 gives tailoring conditions for four binary mixtures of He, A, N_2, and H_2 driving argon; the corresponding P_{21}, P_{41}, T_2, T_5 values and the incident shock Mach numbers. Temperatures and Mach numbers are deduced on a basis of a T_1 of 300°K. The accuracy to which the data are given is greater than that warranted by the ideality assumptions. In practice, it is advisable to check the tailoring by following the pressure history at or near the end of the driven section. If the pressure history indicates that a rarefaction wave is reflected from the contact surface this indicates too much H_2 or He. Conversely, a reflected shock or compression wave indicates too much A or N_2. The highest temperatures in Table 1 are suspect owing to ionization of the argon. Agreement with the values calculated by Palmer and Knox[1] is in all cases better than 1%.

It is interesting to note the effect of the addition of reactant gas to the driven argon. From Eq. (7) it can be seen that tailoring depends on both γ_1 and Cv_1. An increase in Cv_1 alone necessitates a corresponding increase in Cv_4 to keep the E_{14} and E_{32} ratios constant. The result is that the percentage of low molecular weight component must be increased, but the P_{41} ratio is unaffected. A decrease in γ_1 will reduce the temperatures obtained for a given P_{21} ratio and will necessitate a reduction in X and an increase in P_{41}. The overall result of the reactant gas is an increase in P_{41} and either an increase or decrease in X, the effects of increasing Cv and decreasing γ acting in opposite directions.

For example, with argon being driven by a H_2-N_2 mixture at a P_{21} ratio of 8, the mole percentage of H_2 is 67.8. If the driven gas is 10% methane in argon the H_2 content must be increased to 69.9% and the P_{41} ratio from 32.6 to 33.7. If

Table 1

	(H_2 – N_2)		(H_2 – A)		(He – N_2)		(He – A)				Mach
P_{21}	X_{H_2}	P_{41}	X_{H_2}	P_{41}	X_{He}	P_{41}	X_{He}	P_{41}	T_2	T_5	no.
2	...	...	0.369	3.67	...	...	0.457	3.67	400.1	513.6	1.34
3	0.230	7.36	0.526	7.34	0.296	7.35	0.630	7.31	484.9	706.8	1.61
4	0.391	11.70	0.619	11.67	0.494	11.66	0.726	11.59	565.1	893.9	1.84
5	0.498	16.51	0.682	16.46	0.619	16.39	0.789	16.29	643.3	1078	2.05
6	0.574	21.66	0.728	21.58	0.704	21.44	0.833	21.31	720.6	1262	2.24
7	0.633	27.06	0.763	26.96	0.767	26.70	0.866	26.56	797.3	1444	2.41
8	0.678	32.64	0.792	32.54	0.815	32.13	0.892	31.98	873.6	1626	2.57
9	0.715	38.38	0.815	38.26	0.853	37.69	0.913	37.54	949.6	1807	2.72
10	0.746	44.25	0.834	44.10	0.883	43.35	0.930	43.20	1025	1989	2.86
12	0.794	56.24	0.864	56.09	0.929	54.91	0.957	54.78	1177	2351	3.13
14	0.830	68.50	0.887	68.33	0.962	66.68	0.977	66.59	1328	2712	3.38
16	0.857	81.00	0.905	80.79	0.987	78.61	0.992	78.57	1479	3074	3.61
18	0.879	93.57	0.920	93.38	...	...	...	...	1629	3435	3.82
20	0.897	106.3	0.931	106.1	...	...	...	...	1780	3796	4.02
25	0.931	138.4	0.953	138.2	...	...	...	...	2156	4699	4.49
30	0.953	170.7	0.969	170.6	...	...	...	...	2532	5601	4.92
40	0.983	236.0	0.988	236.0	...	...	...	...	3284	7405	5.67
50	1.000	301.7	1.000	301.7	...	...	...	...	4035	9208	6.34

the reactant gas is 10% butane the H_2 content must be reduced to 63.2%, and the corresponding P_{41} ratio is 37.7.

References

[1] Palmer, H. B. and Knox, B. E., "Contact surface tailoring in a chemical shock tube," ARS J. **31**, 826–828 (1961).

[2] Glass, I. I. and Hall, J. G., "Shock tubes," *Handbook of Supersonic Aerodynamics* (US Government Printing Office, Washington, D. C., 1959), Sec. 18; also NAVORD Rept. 1488, Vol. 6.

Computing Temperature Perturbations on Thin-Skin Panels

FREDERIC S. BRUNSCHWIG*
The Boeing Company, Seattle, Washington

Nomenclature

$\dot{Q}$ = incident heat flux = $\sigma\epsilon_i T_0^4$
T_a = surface temperature = $T_a(r)$
T_0 = radiation equilibrium temperature
T_s = sink temperature
a = skin thickness
k = skin thermal conductivity
k_1 = rivet conductivity
k_2 = insulation conductivity
r_1 = rivet radius
ϵ_i = surface emittance
σ = Stefan-Boltzmann constant

UNDER aerodynamic heating, a time-dependent perturbation in uniform panel-surface temperature appears at the site of a rivet or thermocouple attachment (Fig. 1). Perturbation due to thermocouple attachment is computed by Beck and Hurwicz[1] for the case of an insulated thermocouple sunk in a conduction medium. For a panel constructed of a thin metal skin backed by insulation, or open to radiate to a sink, the perturbation for given incident heat flux and rear-structure temperature is determined at any time. The steady-state heat flow equation is set up in cylindrical coordinates on the skin by setting the incident heat flux less the forward and backward reradiated heat fluxes equal to the net radial heat conduction for an annulus[2]:

$$ak\left(\frac{d^2T_a}{dr^2} + \frac{1}{r}\frac{dT_a}{dr}\right) + \dot{Q} - \sigma\epsilon_i T_a^4 - k_i(T_a - T_s) = 0 \tag{1}$$

where $i = 1$ for $0 \leq r \leq r_1$, and $i = 2$ for $r_1 \leq r \leq r_2$.

The term $k_i(T_a - T_s)$ represents heat conducted to the sink through insulation. If the skin is open to reradiate to a sink, then one approximates this heat by letting $k_i = 4\sigma\epsilon_i T_s^3$ for $T_a \sim T_s$.

The substitutions

$$T_a = T_0 - T_i \qquad T_s = T_0 - T_g \tag{2}$$

will produce a differential equation for the perturbation. T_i is the perturbation and T_g is the temperature difference between radiation equilibrium and the sink. Substituting Eq. (2) in Eq. (1) and dropping terms higher than the first power of T_i in the expansion

$$T_a^4 = T_0^4 - 4T_0^3T_i + 6T_0^2T_i^2 - 4T_0T_i^3 + T_i^4 \tag{3}$$

since $T_i/T_0 \ll 1$,

$$(d^2T_i/dr^2) + (1/r)(dT_i/dr) + \lambda_i^2T_i = B_i\lambda_i^2 \qquad i = 1, 2 \tag{4}$$

Received January 14, 1963.

* Research Engineer, Physics Technology.

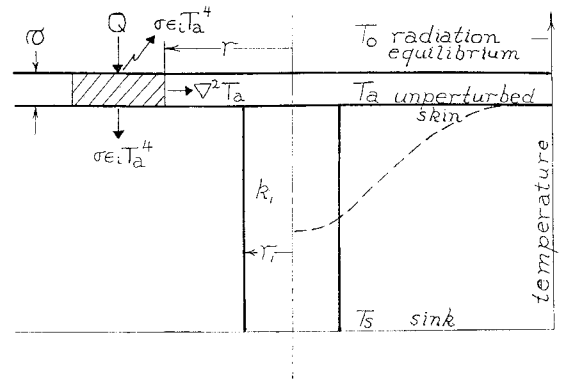

Fig. 1 Thermocouple or rivet attachment to thin-skin panel configuration with a typical temperature perturbation indicated by the dashed line.

where

$$\lambda_i^2 = -(4\sigma\epsilon_i T_0^3 + k_i)/ak \qquad B_i = -k_i T_G/\lambda_i^2 ak \tag{5}$$

The solution to Eq. (4) is of Bessel functions of the first and second kinds with imaginary argument:

$$T_1(r) = AJ_0(j\lambda_1 r) + B_1 \qquad \text{for } 0 \leq r \leq r_1 \tag{6}$$

and

$$T_2(r) = CJ_0(j\lambda_2 r) + DY_0(i\lambda_2 r) + B_2 \qquad \text{for } r_1 \leq r \leq r_2 \tag{7}$$

The boundary conditions are at $r = r_1$, $T_1 = T_2$ and $dT_1/dr = dT_2/dr$, and at $r = r_2$

$$T_2 = -k_2 T_G/(4\sigma_2 T_0^3 + k_2)$$

One assumes $r_2 \geq 10\ r_1$, that is, the perturbation has disappeared at 10 rivet radii. Equations (6) and (7) are solved subject to the boundary conditions simultaneously for the constants. Should $T_1(0)$ be an appreciable fraction of T_0, then an iteration must be performed by including in λ_1^2 the necessary terms of Eq. (3) evaluated for average value of T_1 between $r = 0$ and $r = r_1$ and by iterating Eq. (4) to obtain a new perturbation temperature distribution. The perturbation temperature is large only when $T_s \ll T_0$.

In this case, since the temperature gradient to the sink is assumed linear, one must be sure that the sink temperature is chosen appropriately close to the surface (at the rivet shank for a $\frac{1}{4}$-in.-long rivet) to insure sufficient accuracy.

The perturbation first increases with increasing heat flux, reaches a maximum, and then decreases. This phenomenon occurs whether the sink temperature is constant or follows the surface-temperature increase (Fig. 2).

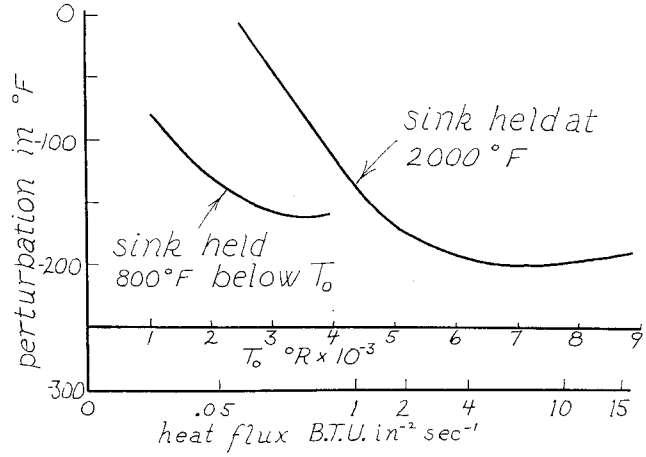

Fig. 2 Temperature perturbation at $r = 0$ as a function of heat flux.